THE ASTROPHYSICAL JOURNAL, 498:L75–L78, 1998 May 1
© 1998. The American Astronomical Society. All rights reserved. Printed in U.S.A.

ISOTOPIC COMPOSITION OF SOLAR WIND CALCIUM: FIRST IN SITU MEASUREMENT BY CELIAS/MTOF ON BOARD *SOHO*

R. KALLENBACH,[1] F. M. IPAVICH,[2] P. BOCHSLER,[3] S. HEFTI,[3] P. WURZ,[3] M. R. AELLIG,[3] A. B. GALVIN,[2] J. GEISS,[1] F. GLIEM,[4] G. GLOECKLER,[2] H. GRÜNWALDT,[5] M. HILCHENBACH,[5] D. HOVESTADT,[6] AND B. KLECKER[6]

Received 1997 November 24; accepted 1998 February 6; published 1998 April 7

ABSTRACT

We present the first results of the Ca isotopic abundances derived from the high-resolution Mass Time-of-Flight (MTOF) spectrometer of the Charge, Element, and Isotope Analysis System (CELIAS) experiment on board the *Solar and Heliospheric Observatory* (*SOHO*). We obtain the isotopic ratios $^{40}Ca/^{42}Ca = 128 \pm 47$ and $^{40}Ca/^{44}Ca = 50 \pm 8$, consistent with terrestrial values. This is the first in situ determination of the solar wind calcium isotopic composition and is important for studies of stellar modeling and solar system formation since the present-day solar Ca isotopic abundances are unchanged from their original isotopic composition in the solar nebula.

Subject headings: solar system: formation — Sun: abundances — Sun: solar wind

1. INTRODUCTION

The main motivation for studying solar wind composition is to obtain information on the isotopic composition of elements in the Sun. This is important because the Sun constitutes 99.9% of solar system matter, and for most elements the solar composition could provide the most reliable information on the composition of the primordial solar nebula. Because nowhere in the Sun have temperatures ever been high enough to alter isotopic abundances of heavy elements by nuclear reactions, solar Ca is thought to reflect the original isotopic composition in the solar nebula. Yet most of what is known of solar isotopic abundances is inferred from terrestrial and from meteoritic abundances with a few exceptions: recently, the isotopic composition of solar wind magnesium, the first analysis of the isotopic abundances of a refractive element in solar matter measured in situ with the High Mass Resolution Spectrometer (MASS) on board *WIND*, has been reported (Bochsler et al. 1995). The solar isotopic composition of the volatile noble gases helium and neon have been determined in situ with the *Apollo* foil experiments (Geiss et al. 1972). In situ measurements with the Charge, Element, and Isotope Analysis System/Mass Time of Flight (CELIAS/MTOF) (Kallenbach et al. 1997) on board the *Solar and Heliospheric Observatory* (*SOHO*) spacecraft have confirmed that the solar neon isotopic composition differs significantly from the terrestrial and meteoritic abundances. Isotopic abundances have also been determined for several elements (C, N, O, He, Ne, Mg) in the higher energy (above 10 MeV amu^{-1}) solar energetic particles (Leske et al. 1996; Mason, Mazur, & Hamilton 1994; Mewaldt, Spalding, & Stone 1984; Selesnick et al. 1993). From similar measurements, it has been possible to obtain reliable information on coronal elemental abundances, including the abundance of calcium (Breneman & Stone 1985). However, the isotopic composition of solar energetic particles may not be representative of the solar composition because fractionation processes occur during particle acceleration and transport and because these processes may vary from event to event. The far more fluent solar wind is the most authentic sample of the solar source composition. From recent theoretical models (e.g., Bodmer & Bochsler 1996), it is expected that the isotopic fractionation in the solar wind flow due to differences in Coulomb drag depletes the heavier isotopes by at most a few percent. Therefore, measurements of the solar wind isotopic abundances of the heavy element calcium, together with previous measurements of magnesium abundances, provide additional evidence that the solar isotopic composition of refractive elements agrees with terrestrial and meteoritic values.

2. INSTRUMENTATION

The MTOF sensor (Fig. 1) of CELIAS on board *SOHO* is an isochronous time-of-flight mass spectrometer (Hovestadt et al. 1995) with a resolution $M/\Delta M$ of better than 100. This provides the possibility of resolving the different isotopes of almost all solar wind elements in the range 3–60 amu. The instrument detects ions at solar wind bulk velocities of 300–1000 km s^{-1}, corresponding to energies of about 0.3–3 keV amu^{-1}. Details on the principle of operation, the calibration of the instrument functions, and the format of the data transferred by the telemetry can be found in the initial publication of CELIAS/MTOF isotope abundance measurements of solar wind neon (Kallenbach et al. 1997). Here we only briefly describe the instrument characteristics that are necessary to understand the quantitative evaluation of time-of-flight (TOF) spectra.

Highly charged solar wind ions enter the instrument (Fig. 1) through the Wide Angle Variable Energy (WAVE) entrance system, which has an energy-per-charge (E/q) acceptance bandwidth of about half a decade and a conic field of view of $\pm 25°$ width (Hovestadt et al. 1995). All calcium isotopes have approximately the same bulk velocity, the same charge state, and the same width of the drifting Maxwellian velocity distribution, so that the heavier isotopes have a higher center E/q. The strongest instrumental fractionation occurs when the center E/q of either isotope coincides with one of the edges of the E/q acceptance of the WAVE. The acceptance

[1] International Space Science Institute, Hallerstrasse 6, CH-3012 Bern, Switzerland; reinald.kallenbach@issi.unibe.ch.
[2] Department of Physics and Astronomy, University of Maryland, College Park, MD 20742.
[3] Physikalisches Institut, University of Bern, CH-3012 Bern, Switzerland.
[4] Institut für Datenverarbeitungsanlagen, Technische Universität, Postfach 20, D-38106 Braunschweig, Germany.
[5] Max-Planck-Institut für Aeronomie, D-37189 Katlenburg-Lindau, Germany.
[6] Max-Planck-Institut für extraterrestrische Physik, Postfach 1603, 85740 Garching bei München, Germany.

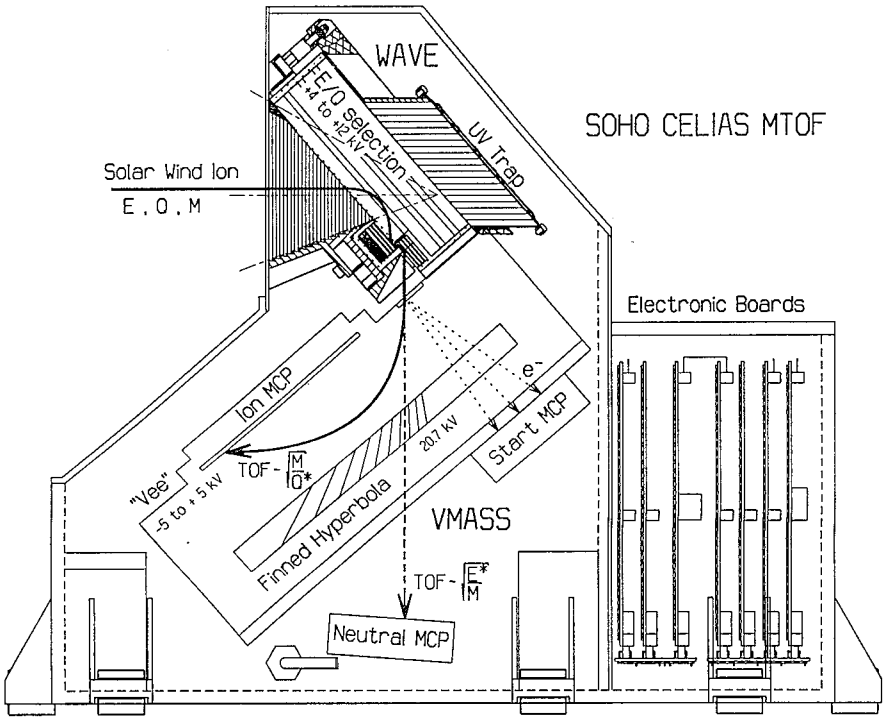

FIG. 1.—Schematic view of the *SOHO*/CELIAS/MTOF sensor

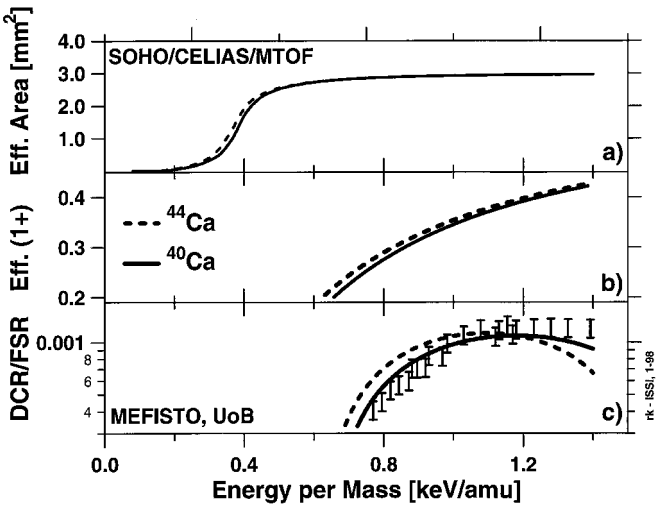

FIG. 2.—$^{40}Ca/^{44}Ca$ detection efficiencies of MTOF. (*a*) Front secondary electron detection assembly rate (FSR) model functions vs. energy per mass in units of mm^2 representing the effective detection area of the CELIAS/MTOF sensor at optimum orientation and energy-per-charge acceptance. (*b*) Illustration of the probability that the ^{40}Ca and ^{44}Ca isotopes leave the foil singly ionized. Most particles leave the carbon foil at the entrance of the isochronous TOF spectrometer VMASS as neutrals or singly charged. (*c*) Ratio of the DCR of $^{40}Ca^+$ and $^{44}Ca^+$ over the FSR vs. ion energy per mass: the calibration data from the MEFISTO ion source at UoB (Marti 1997) are described by a model that includes charge exchange processes, energy loss, and straggling, including its corresponding angular scattering in the carbon foil, ion optics, and the stop detector efficiency. At low energies, $^{44}Ca^+$ has a higher chance of being detected than $^{40}Ca^+$ because the heavier isotope suffers less angular straggling, whereas at higher energies, $^{44}Ca^+$ has a higher risk of overshooting the IMCP or hitting the hyperbola deflection electrode than $^{40}Ca^+$ because the heavier particle suffers less energy loss.

function, including the ion optical effects of the postacceleration voltage to the time-of-flight section, has been well analyzed in the calibration system for mass spectrometers (Steinacher, Jost, & Schwab 1995; Kallenbach et al. 1997) of the University of Bern (UoB). Therefore, the flight data can be reliably filtered with respect to the ion optical instrument discrimination for any element or isotope detected in the solar wind. A much weaker instrumental fractionation is due to the element-specific detection efficiencies of the VMASS subsystem, which is a V-shaped isochronous time-of-flight spectrometer (Hovestadt et al. 1995). The ratio of the double coincidence rate (DCR) over the front secondary electron detection assembly rate (FSR) has been measured as a function of ion energy per mass with a $^{40}Ca^{4+}$ beam of the MEFISTO laboratory at UoB (Marti 1997). The model functions reproduce the calibration data very well, so that they can be applied to derive the differences in the detection efficiencies of the isotopes ^{40}Ca, ^{42}Ca, and ^{44}Ca (Fig. 2). The uncertainty of these detection efficiencies can be assumed to be lower than the statistical error evaluated with very good confidence (see Table 1).

3. DATA ANALYSIS

Figure 3 shows a spectrum where all pulse-height analysis data of the full year 1996 have been collected in the mass range 39–45 amu. TOF channel contents have been put into bins six channels wide, and the uncertainties of the data points have been estimated by the linear optimization algorithm of Rauch-Tung-Striebel (Gelb et al. 1974), where the filter width corresponds to half the TOF resolution of the instrument; this filter introduces a minor reduction of the peak resolution of 12%. This algorithm has been applied to improve the signal-to-noise

TABLE 1

FITTED PARAMETERS OF THE MODEL FUNCTION (EQ. [1]) FOR THE CALCIUM PULSE-HEIGHT ANALYSIS SPECTRUM

	A_i			TOTAL COUNTS	
ION	(10+)[a]	(11+)[b]	p_i[c]	(10+)[a]	(11+)[b]
$^{40}Ca^+$	9756 ± 42	9600 ± 41	3053.1	58289 ± 251	57357 ± 245
$^{42}Ca^+$	98 ± 25	68 ± 17	3128.4	585 ± 149	406 ± 102
$^{43}Ca^+$	14 ± 14	11 ± 11	3165.5	84 ± 84	66 ± 66
$^{44}Ca^+$	218 ± 18	183 ± 15	3203.9	1302 ± 108	1093 ± 90
$^{39}K^+$	148 ± 14	103 ± 12	3014.6	884 ± 84	615 ± 72
$^{41}K^+$	11 ± 11	7 ± 7	3091.0	64 ± 64	45 ± 45

NOTE.—The 1 σ errors of the amplitudes are determined with the maximum likelihood method. The parameters that are equal for all isotopes and for both assumptions of 10- and 11-fold–charged solar wind calcium have been fitted as $s = 9.222$, $b_1 = 0.023$, $b_2 = 0.009$, $b_3 = 0.047$, $b_4 = 0.178$, $b_5 = 0.117$, $l = 9.454$, and $w = 10.146$. The values for the ringing peaks have been taken from the neon evaluations and kept fixed: $c = 0.035$, $r = 31.66$, and $u = 5.71$.

[a] Data reduction based on the assumption of 10-fold–charged solar wind calcium.

[b] Data reduction based on the assumption of 11-fold–charged solar wind calcium.

[c] Fixed calibrated relative peak positions with fitted offset to match spectrum of flight data.

ratio by a factor of 4, so that $^{42}Ca^+$ and $^{44}Ca^+$ can be identified with high significance. Note that most incident ions leave the carbon foil as neutrals or singly charged. The $^{40}Ca^+$ distribution is asymmetrically broadened. It exhibits a different shape than $^{20}Ne^+$ (Kallenbach et al. 1997) for one main reason: singly charged calcium generally has much higher E/q inside the VMASS than singly charged neon, so that calcium follows a longer trajectory in the field-free region above the ion stop microchannel plate (IMCP) detector (Hovestadt et al. 1995). Longer trajectories in the field-free region correspond to longer times of flight. This leads to the tails of higher channels in the TOF distribution of all the mass peaks in Figure 3. As in the case of $^{20}Ne^+$, $^{21}Ne^+$, and $^{22}Ne^+$ (Kallenbach et al. 1997), the electronic ringing peaks are visible at about 30 TOF channels to the left of the $^{40}Ca^+$, $^{42}Ca^+$, and $^{44}Ca^+$ signatures; they arise from reflected start signals. The TOF counts have been weighted by the detection efficiencies for the different calcium isotopes within the window of ±15% instrument fractionation between $^{44}Ca^+$ and $^{40}Ca^+$. All three detectable calcium peaks, $^{40}Ca^+$, $^{42}Ca^+$, and $^{44}Ca^+$, are described by the same model function with identical asymmetric shape. Also, the marginally detectable or nondetectable peaks $^{39}K^+$, $^{41}K^+$, and $^{43}Ca^+$ are included in the fit function, assuming terrestrial isotopic abundances:

$$F(t) = \sum_{i=39}^{44} A_i \left\{ \exp\left[-\frac{(t - p_i)^2}{2s^2} \right] \right\} + \sum_{j=1}^{5} b_j \Big/ \left[1 + \frac{(t - p_i - jl)^2}{w^2} \right] + c \left\{ \exp\left[-\frac{(t - p_i + r)^2}{2u^2} \right] \right\}, \quad (1)$$

with t the time-of-flight channel number and the free fit parameters A_{40}, A_{42}, and A_{44} representing the amplitudes of the $^{40}Ca^+$, $^{42}Ca^+$, and $^{44}Ca^+$ peaks, p_{40} the main Gaussian peak position of $^{40}Ca^+$, l the shift of the Lorentzians describing the asymmetry against the main Gaussians for all three peaks of $^{40}Ca^+$, $^{42}Ca^+$, and $^{44}Ca^+$, r the shift of the ringing peaks against the main Gaussians, b_j the relative amplitudes of the shifted Lorentzians compared with the main Gaussians, c the relative amplitude of the ringing peaks, s the width of the main Gaussian peaks, w the width of the Lorentzian peaks, and u the width of the ringing peaks. The Gaussian peak positions p_{39}, p_{41}, p_{42}, p_{43}, and p_{44} of $^{39}K^+$, $^{41}K^+$ and $^{42}Ca^+$, $^{43}Ca^+$, and $^{44}Ca^+$ are kept fixed at their calibrated TOF channels. The total amplitudes A_{40}, A_{42}, and A_{44}, the widths w and u, and the relative amplitudes b_j give the abundances for $^{40}Ca^+$, $^{42}Ca^+$, and $^{44}Ca^+$. This analysis has been done twice assuming that the solar wind calcium is either 10-fold or 11-fold charged. Table 1 lists the integrated counts for $^{40}Ca^+$, $^{42}Ca^+$, and $^{44}Ca^+$ assuming 10-fold–charged solar wind calcium. This gives the count ratios $^{40}Ca^+/^{42}Ca^+ = 100 \pm 25$ and $^{40}Ca^+/^{44}Ca^+ = 45 \pm 4$. Analogously, assuming 11-fold–charged solar wind calcium, we find $^{40}Ca^+/^{42}Ca^+ = 141 \pm 36$ and $^{40}Ca^+/^{44}Ca^+ = 53 \pm 4$. We further correct these ratios for the effect of heavy elements such as Si and Fe having different mean velocities in the solar wind compared with the proton velocity v_H derived from the proton monitor data (Ipavich et al. 1998). For Ca, the mean velocity can be estimated to be $1.027v_H - 14.6$ km s^{-1} (Hefti 1997). This correction in the mean velocity and therefore in the mean

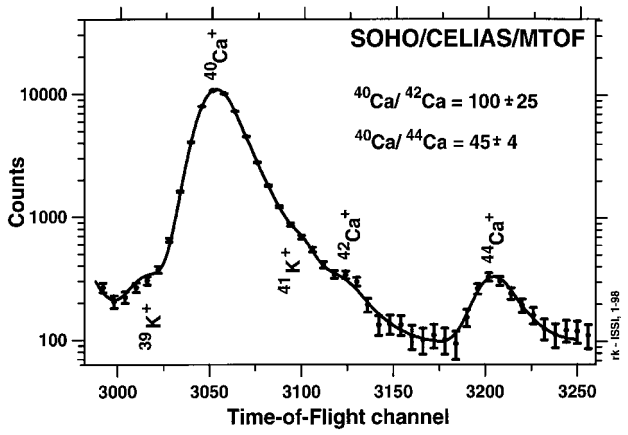

FIG. 3.—TOF spectrum derived from the pulse-height analysis data of the full year 1996 filtered with respect to instrument fractionation with a window of ±15%. A background of 1500 counts has been subtracted in the diagram but has been included in the error estimation with the linear-optimization algorithm of Rauch-Tung-Striebel (Gelb et al. 1974). The solid line represents the fitted model function of the TOF response. The analysis shown here assumes that the solar wind calcium always entered the instrument 10-fold charged. The same analysis has been redone assuming 11-fold–charged solar wind calcium (see text).

TABLE 2

RESULTS FROM MEASUREMENTS OF THE TERRESTRIAL, SOLAR, AND PRESOLAR CALCIUM ISOTOPIC COMPOSITION

$^{40}Ca/^{44}Ca$	$^{40}Ca/^{42}Ca$	Source	Reference
47.153 ± 0.003	151.04 ± 0.02	Terrestrial	1
45.1 ± 0.8	147 ± 2	Average of presolar grains	2
2.3 ± 0.2	...	Presolar X-grain	3
50 ± 8	128 ± 47	Solar wind (*SOHO*/CELIAS)	4

REFERENCES.—(1) Russell et al. 1977; (2) Amari, Zinner, & Lewis 1996; (3) Hoppe et al. 1996; (4) this work.

E/*q* leads to the values $^{40}Ca^{+}/^{42}Ca^{+} = 107 \pm 25$ and $^{40}Ca^{+}/^{44}Ca^{+} = 46 \pm 4$ for 10-fold–charged solar wind calcium and $^{40}Ca^{+}/^{42}Ca^{+} = 148 \pm 36$ and $^{40}Ca^{+}/^{44}Ca^{+} = 54 \pm 4$ for 11-fold–charged solar wind calcium. According to Aellig et al. (1998) and O. Kern (1997, private communication), the coronal freeze-in temperatures for the time period considered in this Letter are such that the average solar wind calcium charge state should be somewhere between 10 and 11; the average number is approximately 10.5. Therefore, the final values for the solar wind calcium isotopic abundance ratios are taken as the average of the two values derived for the two assumptions of 10-fold and 11-fold calcium. The error of the mean value is chosen sufficiently large to be compatible with both assumptions. For all ratios, an additional uncertainty of 4% is due to uncertainties in the absolute calibration of the instrument acceptance. This results in $^{40}Ca^{+}/^{42}Ca^{+} = 128 \pm 47$ and $^{40}Ca^{+}/^{44}Ca^{+} = 50 \pm 8$. More precise values can be determined, once the charge distribution of solar wind calcium is better known for the year 1996 with other instrumentation on board the *SOHO* spacecraft. The sensors *WIND*/MASS and CELIAS/MTOF will provide sufficient information to reevaluate the calcium data.

4. RESULTS

Based on the assumption that the solar wind calcium charge state varies between 10 and 11 as a long-term average, we find that the isotopic abundance ratios of solar wind calcium are $^{40}Ca/^{42}Ca = 128 \pm 47$ and $^{40}Ca/^{44}Ca = 50 \pm 8$. Both ratios are consistent with the terrestrial ratios $^{40}Ca/^{42}Ca = 151.04 \pm 0.02$ and $^{40}Ca/^{44}Ca = 47.153 \pm 0.003$ (Russell et al. 1977). More precise values can be obtained once a time series during the year 1996 of the calcium charge states in the solar wind at the *SOHO* location is available.

5. DISCUSSION

From astrophysical and geochemical considerations, it can be concluded that the isotopic composition of photospheric Ca must be within small fractions per mil identical to the terrestrial composition. The similarity of the solar wind results with the terrestrial values suggests the preliminary conclusion that isotopic fractionation within the solar wind plays a minor role. This is supported by the model calculations of Bodmer & Bochsler (1996) that consider differences in the Coulomb drag for isotopes of various elements. Fractionation effects not larger than a few percent are expected for Ne and Mg. For the heavy element Ca, even weaker isotopic fractionation has to be expected. Although there are as yet no detailed evaluations of a more extensive time series with calcium isotopic ratios to be determined in different solar wind regimes, we suggest that the Ca abundance discussed in this work is within a few percent of the true solar composition.

Table 2 shows a comparison between the terrestrial, solar, and presolar grain calcium isotopic composition. There is no evidence for large variations in these isotopic compositions, except for the case of the presolar X-grains that originate from supernovae explosions (Hoppe et al. 1996; Nittler et al. 1996). The large enrichment in ^{44}Ca in the X-grains is a consequence of the radioactive decay of ^{44}Ti in supernovae material.

This work was supported by the Swiss National Science Foundation, by the PRODEX program of ESA, by NASA grant NAG5-2754, and by DARA, Germany, with grants 50 OC 89056 and 50 OC 9605. The flight-spare unit of MTOF has been recalibrated with the electron cyclotron resonance ion source in the MEFISTO laboratory at the University of Bern and with the support of Adrian Marti and Reto Schletti.

REFERENCES

Aellig, M., et al. 1998, J. Geophys. Res., in press
Amari, S., Zinner, E., & Lewis, R. S. 1996, Lunar Planet. Sci., 27, 23
Breneman, H. H., & Stone, E. C. 1985, ApJ, 299, L57
Bochsler, P., Gonin, M., Sheldon, R. B., Zurbuchen, T., Gloeckler, G., Hamilton, D. C., Collier, M. R., & Hovestadt, D. 1995, in Proc. Eighth Int. Solar Wind Conf., ed. D. Winterhalter, J. T. Gosling, S. R. Habbal, W. S. Kurth, & M. Neugebauer (Woodbury: AIP), 199
Bodmer, R., & Bochsler, P. 1996, paper presented at 21st General Assembly of the European Geophysical Society, The Hague, Netherlands, 1996 May 6–10
Geiss, J., Bühler, F., Cerutti, H., Eberhardt, P., & Filleux, C. 1972, *Apollo 16* Preliminary Scientific Report (SP-315; Washington, DC: NASA), 14.1
Gelb, A., Kasper, J. F., Nash, R. A., Price, C. F., & Sutherland, A. A. 1974, in Applied Optimal Estimation, ed. A. Gelb (Cambridge: MIT Press), 159
Hefti, S. 1997, Ph.D. thesis, Univ. Bern
Hoppe, P., Strebel, R., Eberhardt, P., Amari, S., & Lewis, R. S. 1996, Science, 272, 1314
Hovestadt, D., et al. 1995, Sol. Phys., 162, 441
Ipavich, F. M., et al. 1998, J. Geophys. Res., in press
Kallenbach, R., et al. 1997, J. Geophys. Res., 102, 26895
Leske, R. A., Mewaldt, R. A., Cummings, A. C., Cummings, J. R., Stone, E. C., & von Rosenvinge, T. T. 1996, Space Sci. Rev., 78, 149
Marti, A. 1997, Ph.D. thesis, Univ. Bern
Mason, G. M., Mazur, J. E., & Hamilton, D. C. 1994, ApJ, 425, 843
Mewaldt, R. A., Spalding, J. D., & Stone, E. C. 1984, ApJ, 280, 892
Nittler, L. R., Amari, S., Zinner, E., Woosley, S. E., & Lewis, R. S. 1996, ApJ, 462, L31
Russell, W. A., Papanastassiou, D. A., Tombrello, T. A., & Epstein, S. 1977, in Proc. Eighth Lunar Sci. Conf., Comp. Lunar Science Institute (New York: Pergamon), 3791
Selesnick, R. S., Cummings, A. C., Cummings, J. R., Leske, R. A., Mewaldt, R. A., Stone, E. C., & von Rosevinge, T. T. 1993, ApJ, 418, L45
Steinacher, M., Jost, F., & Schwab, U. 1995, Rev. Sci. Instrum., 66, 4180